



## **New analytical model for viscous wall damper based on refined material testing and analysis**

Kazuhiko Sasaki<sup>(1)</sup>, Kazuhiko Kasai<sup>(2)</sup>

<sup>(1)</sup> General staff, Oiles corporation, [k.sasaki@oiles.co.jp](mailto:k.sasaki@oiles.co.jp)

<sup>(2)</sup> Professor, Tokyo Institute of Technology, [kasai@serc.titech.ac.jp](mailto:kasai@serc.titech.ac.jp)

### ***Abstract***

Viscous damper is one of the most widely used velocity-dependent dampers in Japan. It can reduce building responses of wide range of magnitude, such as micro-vibration caused by traffic, moderate and relatively long vibration caused by wind, and intense vibration caused by a major earthquake. The typical viscous damper in Japan is the viscous wall damper (VWD) which has been produced for more than twenty years. It is like the stud installed between the upper and lower beams, and generates damping force by the shearing force of the viscous fluid. Buildings with VWDs showed well-reduced vibration, as evidenced by their responses recorded during the 2011 Tohoku Earthquake.

The data for dynamic properties and analytical model of the VWD were produced many years ago according to the then-current requirements. In order to promote optimal use of the VWD, more detailed property data and more accurate analytical model are necessary. This paper, therefore, explains the writers' recent study involving comprehensive test program of the viscous material and new analytical modeling with significantly enhanced accuracy. They are summarized below:

The past data for the viscous fluid seemed to contain effects of boundary condition of the test apparatus. After many trial and error, the writers have developed the new test method and apparatus that can extract the ideal data of the viscous fluid by creating simple shearing flow condition. Using thus-obtained data, the analytical model and the approximate model for the viscous fluid are developed. The model appears to be accurate over wide range of material strain up to 2,000%, temperature 0 to 40 degree(C), loading frequency 0.1 to 2.5 Hz.

Since the viscous fluid data and corresponding analytical model mentioned above do not contain specific boundary effect, they can readily be used for analytical model of any damper utilizing shearing flow resistance. Accordingly, a new VWD model is formulated by using the viscous fluid model and the flexibility of the fluid container. The VWD model also appears to be accurate, and its response reduction effectiveness will be demonstrated through analysis of the building under small to catastrophic excitations.

*Keywords: analytical model, viscous damper, testing*

## 1. Introduction

### 1.1 Background

Viscous Wall Damper (VWD) is one of the shock absorbers that reduce building's vibration <sup>[1],[2]</sup>. VWD, which is the thin shape and located in the walls of the buildings (Fig.1), can absorb the energy that are small and large amplitude such vibration of wind and earthquake. And it is called that the characteristics of it is depends on the velocity. Recently, the records of buildings response of the 2011 off the Pacific coast of Tohoku Earthquake in Japan showed that the damper depending on the velocity like VWD had more effect to reduce the building's acceleration than the damper depending on the displacement <sup>[3]</sup>.

The characteristics of damper like VWD depending on velocity are often expressed by the nonlinear viscosity formula that is proportional to the exponential of velocity <sup>[1],[2]</sup>. Because the influence of the velocity to the dampers characteristic in the large vibration like the buildings response during earthquakes is larger than other factors. However, in past study, authors studied the characteristics of the viscous fluid material of VWD in detail with the small test equipment, and found that its characteristics are similar to that of viscoelastic material and dependent frequency especially in small vibration (Fig.2) <sup>[4]</sup>. And they proved that the viscoelastic mechanical model could represent characteristics of viscous fluid material in the wide range of frequency (0.1~2.5Hz), amplitude (25~2000%) and temperature (0~40°C) with a high precision <sup>[5],[6]</sup>. In the following, the viscoelastic mechanical model is thing that shows the stress-strain hysteresis loop is a sloping ellipse with frequency dependency.



Fig. 1 – VWD set in building

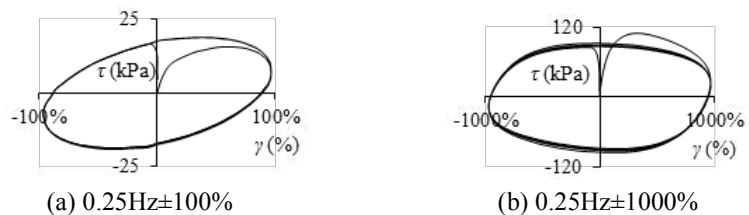


Fig. 2 – Stress-strain hysteresis loops of viscous fluid material of test

Although there are some viscoelastic mechanical models <sup>[1],[7]</sup>, in the study described in above sentence, the fractional derivative model is used. It is one of the models that can calculate shearing forces of viscoelastic materials in time history analysis and considered by Kasai et al <sup>[8]-[11]</sup>. It is model that is an equation with the fractional derivative constitutive law and can calculate the shearing forces of the viscoelastic mechanical model with small number parameters in a high accuracy. However, it is difficult to use it because its equation is more complex than other models. In another study, the simply model depending on the frequency were made, but it was not always practical <sup>[12]</sup>.

The document 1 shows the ability to absorb the damping energy decreases when the constructional elements and joints of the damper are deformed. And the more correct method to calculate the energy is to bind the stiffness of those elements to the dampers model. However, it is more difficult and complex to make the high precision model and use it in time history analysis. Therefore, if the simple model calculated in a high accuracy exists, it considers it can be easier to express the characteristics of such complex constructions and other kinds of materials with frequency dependency.

### 1.2 Purpose

This papers purpose is to make the simple model that can calculate the shearing force of viscoelastic mechanical model with frequency dependent in time history analysis for the viscous damper and the viscoelastic damper. In addition, the calculation accuracy of this model is close to that of the fractional derivative model. The method to make this model is to calculate firstly the instant frequency changing at each step in time history analysis with the equation made from the sine waves logic, and secondly the shearing force of the viscoelastic mechanical model for Kelvin model. Though it is considered that there are many kinds of material depending frequency, this paper shows the method to apply the linear characteristics of 2 kinds of material (viscous fluid and viscoelastic) to the simple model.

## 2. General characteristics of the dampers with viscous fluid or viscoelastic materials

### 2.1 Configuration and installation of the dampers with viscous fluid or viscoelastic materials

Viscous wall damper (VWD) is one of the viscous dampers in Fig.3 (a). There is viscous fluid material filled into shearing gaps between the upper plates and the lower container. It is located between the upper and lower beams of the buildings like a wall and moves in a horizontal direction. In addition, different mounting method, there is the brace type that installs at an angle in the beam-column frame and moves in the axial direction in Fig.3 (c). The characteristics of it are almost same to that of wall type if the viscous fluid material is same.

The viscoelastic damper shown in Fig.3 (b), (d) is similar to the viscous fluid damper in its configuration, force development and joint in building. There is viscoelastic material bonded between some plates. And the dampers are set as a wall or brace type in the buildings. Though the state of the material is difference between solid and liquid, each damper material is between the plates and each damper force is material shearing force.

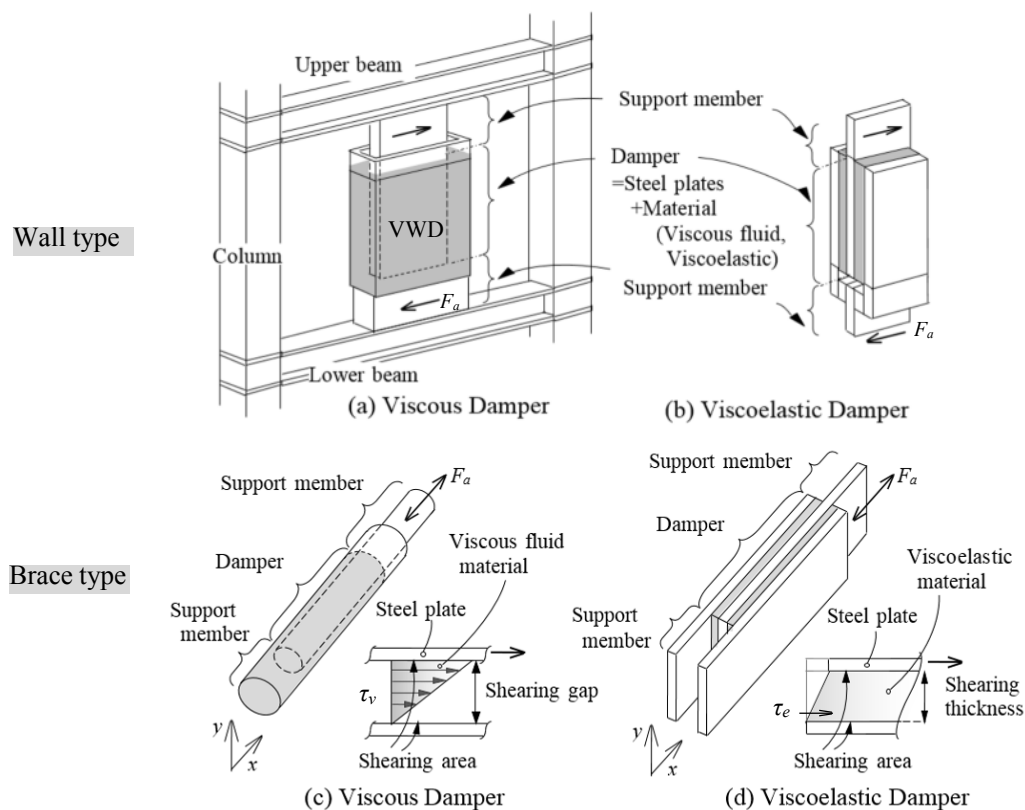


Fig. 3 – Configuration and installation of viscous damper and viscoelastic damper

### 2.2 Basic characteristics of viscoelastic mechanical model

As mentioned in Section 1.1, the viscoelastic mechanical model can be express the characteristics of viscous damper especially in small deformations as well as the viscoelastic damper. In the viscoelastic mechanical, the strain and  $\gamma(t)$  and shearing stress  $\tau(t)$  are Eq. (1a, b) with displacement  $u(t)$ , shearing force  $F(t)$ , shearing gap or thickness  $d$ , and the shearing area  $S$ .

$$\gamma(t) = u(t) / d, \quad \tau(t) = F(t) / S \quad (1a, b)$$

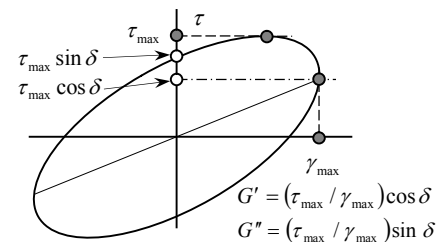


Fig. 4 – Characteristics of viscoelastic mechanical model



The sine wave hysteresis loop of the shearing force  $\tau(t)$  and the strain  $\gamma(t)$  is the inclined ellipse in Fig.4. The sine wave is expressed by the strain  $\gamma(t) = \gamma_{max} \sin \omega t$  with the strain maximum  $\gamma_{max}$ , circular frequency  $\omega$  and time  $t$ .  $\tau(t)$  is expressed by Eq. (2). The Equation has two proportional terms of  $\gamma(t)$  and strain velocity  $\dot{\gamma}(t)$  with the phase difference  $\delta$  and the shearing force max  $\tau_{max}$ . It stands for Kelvin model. The model's characteristic values are the storage (elastic) stiffness modulus  $G'$ , the loss (viscous) stiffness modulus  $G''$ , and the loss factor  $\eta = \tan \delta = G''/G'$ .

$$\begin{aligned} \tau(t) &= \tau_{max} \sin(\omega t + \delta) = \tau_{max} \cos \delta \sin \omega t + \tau_{max} \sin \delta \cos \omega t \\ &= \left( \frac{\tau_{max}}{\gamma_{max}} \cos \delta \right) \gamma(t) + \left[ \left( \frac{\tau_{max}}{\gamma_{max}} \sin \delta \right) / \omega \right] \dot{\gamma}(t) = G' \gamma(t) + \frac{G''}{\omega} \dot{\gamma}(t) \end{aligned} \quad (2)$$

### 2.3 Damping force including the additional stiffness

The storage stiffness  $K'$  and the loss stiffness  $K''$  are expressed by Eq. (3a, b) with a shearing area  $S$  and the shearing gap  $d$  and converted from  $G'$  and  $G''$  of the the previous section.

$$K' = G' \frac{S}{d}, \quad K'' = G'' \frac{S}{d} \quad (3a, b)$$

The damping force  $F_a$  considered the additional stiffness  $K_s$  of the supports and joints members is expressed by the Maxwell model that is the unit of the stiffness of Eq. (3a, b) and  $K_s$  in series. The storage stiffness  $K'_a$  and the loss stiffness  $K''_a$  are expressed by Eq. (4a, b).

$$K'_a = \frac{K_s (K'^2 + K_s K' + K''^2)}{(K' + K_s)^2 + K''^2}, \quad K''_a = \frac{K_s^2 K''}{(K' + K_s)^2 + K''^2} \quad (4a, b)$$

Therefore,  $F_a$  considered with  $K_s$  is expressed by the Eq. (5) with  $u_a$  that is displacement of the damper and the peripheral members.

$$F_a = K'_a u_a + \frac{K''_a}{\omega} \dot{u}_a \quad (5)$$

As with the previous section, if  $K'_a$  and  $K''_a$  are calculated in each calculation step of the time history analysis,  $F_a$  could be calculated by the above formula. However, this paper shows only the previous section of the model.

## 3. Viscoelastic mechanical models of past studies

### 3.1 High precision models with fractional derivative and test values of materials of 2 kinds of dampers

One of the methods that can be calculated the shearing force of the viscoelastic mechanical model in time history analysis is the fractional derivative model that obtained from fractional derivative constitutive law with the strain  $\gamma$ , the stress  $\tau$ , and the fractional differential operator  $D^\alpha (= d^\alpha / dt^\alpha)$  [5], [6], [8]-[11]. In past studies, the linear characteristics of materials of the viscous damper and the viscoelastic damper were modeled in a high accuracy with the equations and methods shown below [5], [8].

Firstly, the characteristics of the material of the viscous dampers are below. The document 5 shows that the storage stiffness modulus  $G'_v$  (kPa) and the loss stiffness modulus  $G''_v$  (kPa) are expressed by following Eq. (6a, b). Their parameters are  $c_1 = 30$  kPa,  $c_2 = 21$  kPa,  $\alpha_1 = 1.153$  and  $\alpha_2 = 0.52$  and decided from test values. The equivalent frequency is  $f_{eq} = \lambda \omega / (2\pi)$  with  $\omega$  and  $\lambda$ .  $\lambda$  is the shift factor that can represent the temperature features and different by the material. Fig.5 shows  $G'_v$ ,  $G''_v$  to  $f_{eq}$  ( $\lambda = 1$  at 20°C).



$$G'_v(\omega) = c_1 c_2 A / (A^2 + B^2),$$

$$G''_v(\omega) = c_1 c_2 B / (A^2 + B^2) \quad (6a, b)$$

$$A = c_1 \omega^{-\alpha_2} \cos(\alpha_2 \pi / 2) + c_2 \omega^{-\alpha_1} \cos(\alpha_1 \pi / 2),$$

$$B = c_1 \omega^{-\alpha_2} \sin(\alpha_2 \pi / 2) + c_2 \omega^{-\alpha_1} \sin(\alpha_1 \pi / 2) \quad (6c, d)$$

The shearing force  $\tau_v$  can be calculated with the constitutive law expressed by Eq. (7) for time history analysis. Fig.6 shows the hysteresis loops of the sine wave and random wave.

$$c_1 D^{\alpha_1} \tau_v(t) + c_2 D^{\alpha_2} \tau_v(t) = c_1 c_2 D^{\alpha_1 + \alpha_2} \gamma(t) \quad (7)$$

Fig.5, 6 are the values measured by test and calculated by the model. And they show that the values calculated with the model almost agree with that of test.

Secondly, the characteristics of the material of the viscoelastic dampers are below. The document 8 shows that the storage stiffness modulus  $G'_e$  (kPa) and the loss stiffness modulus  $G''_e$  (kPa) are expressed following Eq. (8a, b). Their parameters are  $G = 39.2$  kPa,  $a = 5.6 \times 10^{-5}$ ,  $b = 2.1$  and  $\alpha = 0.558$  and decided from test values. Fig. 7 shows  $G'_e$ ,  $G''_e$  to  $f_{eq}$  ( $\lambda = 1$  at  $20^\circ\text{C}$ ).

$$G'_e(\omega) = G \frac{1 + ab\omega^{2\alpha} + (a+b)\omega^\alpha \cos(\alpha\pi/2)}{1 + a^2\omega^{2\alpha} + 2a\omega^\alpha \cos(\alpha\pi/2)},$$

$$G''_e(\omega) = G \frac{(-a+b)\omega^\alpha \sin(\alpha\pi/2)}{1 + a^2\omega^{2\alpha} + 2a\omega^\alpha \cos(\alpha\pi/2)} \quad (8a, b)$$

The shearing force  $\tau_e$  can be calculated with the constitutive law expressed by Eq. (9) for time history analysis. Fig.8 shows the hysteresis loops of the sine wave and random wave.

$$\tau_e(t) + aD^\alpha \tau_e(t) = G[\gamma(t) + bD^\alpha \gamma(t)] \quad (9)$$

Fig. 7, 8 are the values measured by test and calculated by the model. And they show that the values calculated with the model almost agree with that of test too.

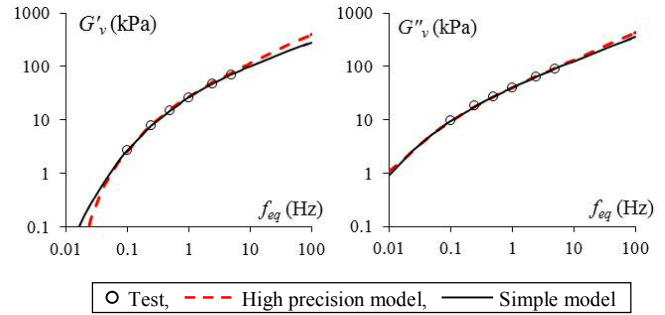


Fig. 5 –  $G'_v$ ,  $G''_v$  -  $f_{eq}$  of test and models (Viscous fluid)

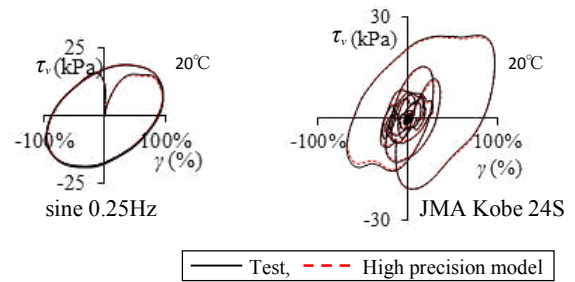


Fig. 6 – Hysteresis loops of test and model (Viscous fluid)

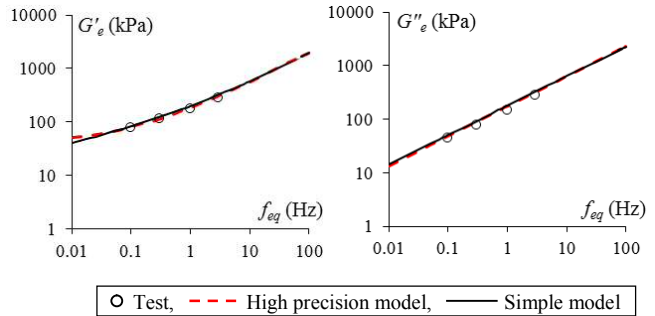


Fig. 7 –  $G'_e$ ,  $G''_e$  -  $f_{eq}$  of test and models (Viscoelastic)

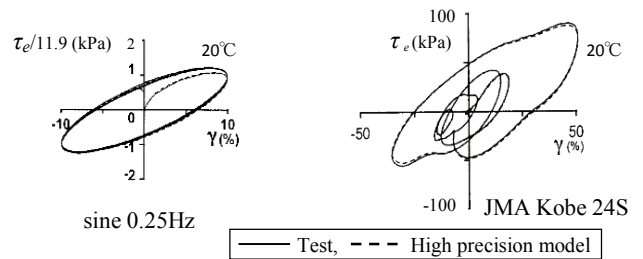


Fig. 8 – Hysteresis loops of test and model (Viscoelastic)



### 3.2 Simple equation of characteristics values with frequency

The relationships between the characteristics values of viscoelastic mechanical model in the previous section and the equivalent frequency  $f_{eq}$  can be simply expressed with Eq. (10a, b), (11a, b) in each damper. However, the shearing force of the viscoelastic mechanical model in time history analysis cannot be calculated with only these equations.

$$G'_v(\omega) = 26 f_{eq}^{(0.43+0.3 f_{eq}^{-0.27})}, \quad G''_v(\omega) = 40 f_{eq}^{(0.46+0.08 f_{eq}^{-0.33})}, \quad f_{eq} = \lambda \omega / (2\pi) \quad (10a, b, c)$$

$$G'_e(\omega) = 185 f_{eq}^{(0.4 f_{eq}^{0.06})}, \quad G''_e(\omega) = 170 f_{eq}^{0.56} \quad (11a, b)$$

In considering the high precision model shown in previous section 3.1, it is more difficult to construct the fractional derivative model and to decide parameters to fit test values, because the equations are more complex and each characteristics values equation have same parameters. On the other hand, it is easier to do with Eq. (10a, b), (11a, b) that because each characteristics value are independent. In time history analysis, if it were possible to calculate  $f_{eq}$  of each calculation step, the characteristics values of Eq. (10a, b), (11a, b) and the shearing force of Eq. (2) would be obtained easily. With the instant circular frequency  $\omega_t$ , the next chapter will show the method to calculate the shearing force in time history analysis.

## 4. Simple model of viscoelastic mechanical model with instant circular frequency

### 4.1 Logical formula of circular frequency in sine wave

Firstly, the method to get the circular frequency  $\omega$  are considered from the logical sine waves Eq. (12a, b, c) of strain  $\gamma$ , strain velocity  $\dot{\gamma}$  and strain acceleration  $\ddot{\gamma}$  with  $\omega$  and the strain maximum  $\gamma_{max}$ .

$$\gamma = \gamma_{max} \sin \omega t, \quad \dot{\gamma} = \gamma_{max} \omega \cos \omega t, \quad \ddot{\gamma} = -\gamma_{max} \omega^2 \sin \omega t \quad (12a, b, c)$$

There are two equations to obtain circular frequency  $\omega$ . One is Eq. (13a, b) with  $\gamma$  and  $\dot{\gamma}$ , the other is Eq. (14a, b) with  $\dot{\gamma}$  and  $\ddot{\gamma}$ .

$$(\omega \cdot \gamma_{max})^2 - (\omega \cdot \gamma)^2 - \dot{\gamma}^2 = 0, \quad \omega = \dot{\gamma} / \sqrt{(\gamma_{max}^2 - \gamma^2)} \quad (13a, b)$$

$$(\omega^2 \cdot \dot{\gamma}_{max})^2 - (\omega \cdot \dot{\gamma})^2 - \ddot{\gamma}^2 = 0, \quad \omega = \sqrt{\dot{\gamma}^2 + \sqrt{\dot{\gamma}^4 + 4(\gamma_{max} \cdot \ddot{\gamma})^2}} / (\sqrt{2} \gamma_{max}) \quad (14a, b)$$

The values required in the time history analysis can change in each calculations step of random waves. It is more important to calculate such  $\omega$  with the relative values like  $\dot{\gamma}$  and  $\ddot{\gamma}$  for the strain  $\gamma$ . So, it is considered to be better to calculate  $\omega$  with Eq. (14b) than Eq. (13b). In addition, 0 do not divide Eq. (14b). Therefore, in the following,  $\omega$  is Eq. (14b) to calculate the shearing force in time history analysis. This  $\omega$  of Eq. (14b) is the instant circulation frequency  $\omega_t$ . In addition, the equation of  $\gamma_{max}$  is deformed from Eq. (13a).

#### 4.2 Calculation precision of instant circle frequency formula with measured values

This section shows the calculation precision of the instant circular frequency  $\omega_t$  calculated by Eq. (14b) with the strain  $\gamma$  measured in sine waves shaking test. Fig.9 (a) is the time history of the strain  $\gamma$  (= displacement / shearing gap) that measured in sine wave that of strain max  $\gamma_{max} = 1$  and frequency  $f = 0.25\text{Hz}$  and Fig.9 (b) is that of the strain acceleration that is difference of  $\gamma$ . It shows that the curve of the strain acceleration is not smooth. In addition, Fig.10 (a) is the time history of  $\gamma_{max}$  with Eq. (13b), and Fig.10 (b) is that of  $\omega$  calculated with Eq. (14b). Both curves are not too smooth to be used for the characteristics model.

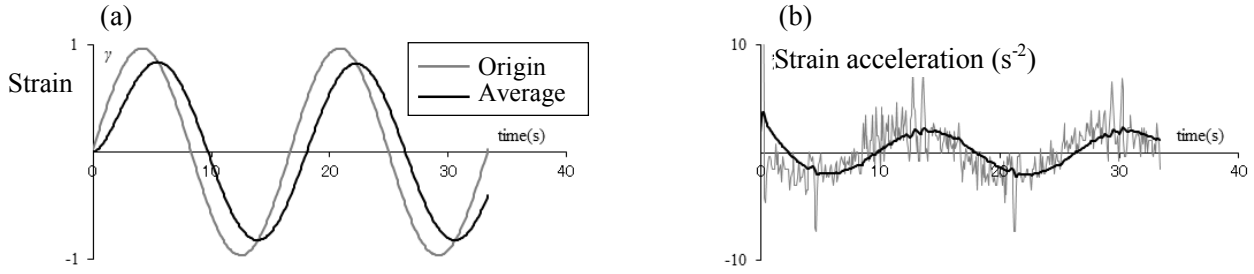


Fig. 9 – Time histories of strain and strain acceleration (sine 0.25Hz)

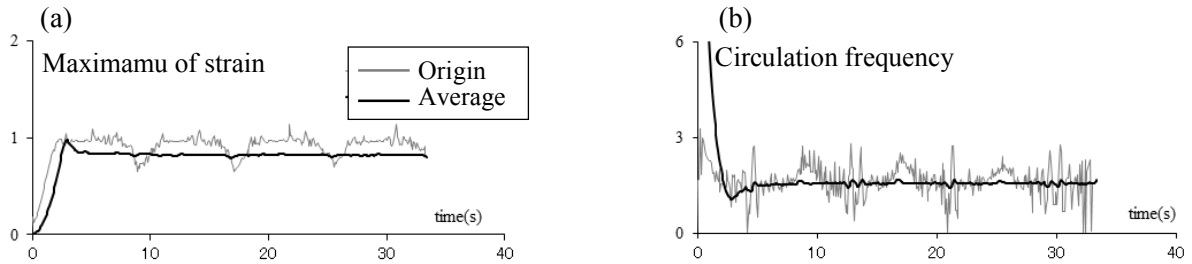


Fig. 10 – Time histories of  $\gamma_{max}$  and  $\omega$  (sine 0.25Hz)

Here, to reduce the fluctuation shown in the Fig.9, 10,  $\omega_t$  is calculated with the average strain  $\gamma_{ave}$  smoothed from  $\gamma$ . The average method is the exponential average of Eq. (15a) that can be easily calculated and reflected by the before steps values. The subscript ( $i$ ) in formula indicates the calculation step number  $i$  and is omitted in the sentence. Eq. (16a, b) are expressed the average strain velocity and the average strain acceleration calculated from the difference of  $\gamma$ .

$$\gamma_{ave}^{(i)} = a_1 \gamma^{(i)} + (1 - a_1) \gamma_{ave}^{(i-1)}, \quad a_1 = 0.05 \cdot 200 f \cdot dt = 10 f \cdot dt \quad (15a, b)$$

$$\dot{\gamma}_{ave}^{(i-1)} = \frac{\gamma_{ave}^{(i)} - \gamma_{ave}^{(i-2)}}{2dt}, \quad \ddot{\gamma}_{ave}^{(i-1)} = \frac{\gamma_{ave}^{(i)} - 2\gamma_{ave}^{(i-1)} + \gamma_{ave}^{(i-2)}}{dt^2} \quad (16a, b)$$

By comparing  $\gamma$  and  $\gamma_{ave}$  in Fig.9 (a), it is found that the smaller the maximum of  $\gamma_{ave}$  is and the larger the delay is, the more smoothly curve is. However, it is considered that the influence of such differences in calculating  $\omega_t$  is small because the fluctuation of  $\omega$  is much smaller than that of  $\gamma$ .

$a_1$  is determined under the condition that values of the simple model are consistent with the target values as much as possible, because characteristics can be different from originals data when  $a_1$  is too small. Here,  $a_1$  is expressed by Eq. (15b) with a frequency  $f$  and the sampling time  $dt$ . It means that  $a_1 = 0.05$  for 200 data per a cycle in sine wave. In the case of random wave,  $f$  assumes to be the dominant frequency.  $\omega_t$  of calculation step ( $i$ ) is expressed by the following Eq. (17). It includes values calculated from the average strain  $\gamma_{ave}$  of calculation step ( $i-1$ ), because  $\omega_t$  does not significantly change.

$$\omega_t^{(i)} = \frac{\sqrt{\dot{\gamma}_{ave}^{(i-1)2} + \sqrt{\dot{\gamma}_{ave}^{(i-1)4} + 4(\gamma_{ave\_max}^{(i-1)} \cdot \dot{\gamma}_{ave}^{(i-1)})^2}}}{\sqrt{2} \gamma_{ave\_max}^{(i-1)}} > 0 \quad (17)$$

In addition,  $\gamma_{ave\_max}$  is the maximum of  $\gamma_{ave}$  and expressed by Eq. (18) that is the deformation of Eq. (13b).

$$\gamma_{ave\_max}^{(i-1)} = \sqrt{(\omega_t^{(i-1)} \cdot \gamma_{ave}^{(i-1)})^2 + \dot{\gamma}_{ave}^{(i-1)2}} / \omega_t^{(i-1)} > 0 \quad (18)$$

Fig.10 (b) shows  $\omega_t$  obtained by Eq. (17). Though there are deference in the initial time,  $\omega_t$  is almost consistent with the logical value  $\omega = 2\pi f = 1.57$ . Therefore, it is considered that the simple model can calculate the shaering force of the viscoelastic mechanical model with Eq. (2), (10), (11), (15) ~ (18).

#### 4.3 Modifying the equation of the shearing force in sine wave

Fig.11 (a) and (b) show 2 kinds materials (viscous fluid and viscoelastic indicated in section 3.2) hysteresis loops calculated with the simple model of previous section and the high precision model of fractional derivative at 20°C. Input data is the sine wave frequency of which is 0.25Hz and  $\gamma_{max}$  of which is 100%. Values of the simple model almost agree with that of the high precision model, but here are the differences in the initial quarter cycle. To confirm this cause, Fig.12 shows the relationship between  $\gamma_{ave} \cdot \dot{\gamma}_{ave}$  and  $\gamma_{ave}$ . It is found that these are larger than 0 in the same range of Fig.11, and such a state does not occur in logical sine wave. So, focusing on this state, this section shows the method to modify the shearing forces  $\tau_v$ ,  $\tau_e$  of 2 materials of viscous fluid and viscoelastic in sine wave.

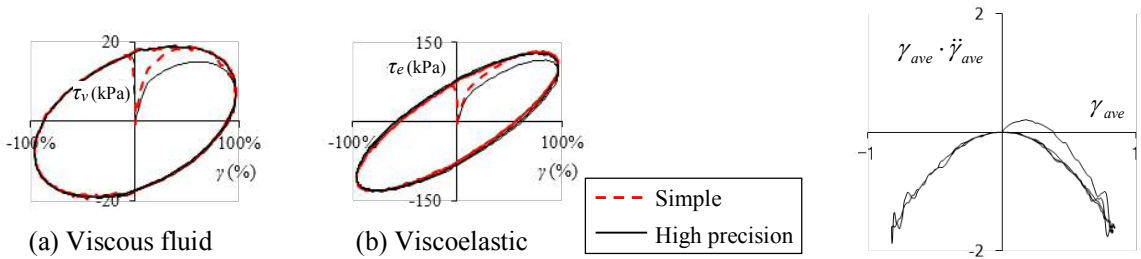


Fig. 11 – Hysteresis loops of each model before modifying (sine 0.25Hz, 20°C)

Fig. 12  $-\gamma_{ave} \cdot \dot{\gamma}_{ave} - \gamma_{ave}$

To modify  $\tau_v$ ,  $\tau_e$  is to use  $\beta_v$ ,  $\beta_e$  expressed by Eq. (19a, b, c) with  $\zeta$  that are the dimensionless of  $\gamma_{ave} \cdot \dot{\gamma}_{ave}$  and expressed by Eq. (20).

$$\beta_v^{(i)} = (1 + 4\zeta^{(i)})^{-1} [\zeta^{(i)} > 0], \quad \beta_e^{(i)} = (1 + 1.5\zeta^{(i)})^{-1} [\zeta^{(i)} > 0], \quad \beta_v^{(i)} = \beta_e^{(i)} = 1 [\zeta^{(i)} \leq 0] \quad (19a, b, c)$$

$$\zeta^{(i)} = \gamma_{ave}^{(i-1)} \cdot \dot{\gamma}_{ave}^{(i-1)} / (\gamma_{ave\_max}^{(i-1)} \cdot \omega_t^{(i-1)})^2 \quad (20)$$

The final  $\tau_v$ ,  $\tau_e$  are expressed by the following Eq. (21), (23). They show that it is the elastic item of Eq. (21), (23) to modify. They have the modifying factor  $\beta_{v\_ave}$ ,  $\beta_{e\_ave}$  to ease the sudden fluctuation of  $\beta_v$ ,  $\beta_e$ . And  $G'_v$ ,  $G''_v$ ,  $G'_e$  and  $G''_e$  are calculated by Eq. (10), (11) with  $\omega_t$ . The average coefficient  $a_2$  is set in the same way as  $a_1$  of Eq. (15b).



Viscous fluid  $\left\{ \begin{array}{l} \tau_v^{(i)} = \beta_{v\_ave}^{(i)} \cdot G_v'(\omega_t^{(i)}) \cdot \gamma^{(i)} + \frac{G_v''(\omega_t^{(i)})}{\omega_t^{(i)}} \cdot \dot{\gamma}^{(i)} \\ \beta_{v\_ave}^{(i)} = \beta_v^{(i)} \cdot \gamma^{(i)} + (1 - a_2) \cdot \beta_{v\_ave}^{(i-1)}, \quad a_2 = 20 f \cdot dt \end{array} \right. \quad (21)$

Viscoelastic  $\left\{ \begin{array}{l} \tau_e^{(i)} = \beta_{e\_ave}^{(i)} \cdot G_e'(\omega_t^{(i)}) \cdot \gamma^{(i)} + \frac{G_e''(\omega_t^{(i)})}{\omega_t^{(i)}} \cdot \dot{\gamma}^{(i)} \\ \beta_{e\_ave}^{(i)} = \beta_e^{(i)} \cdot \gamma^{(i)} + (1 - a_2) \cdot \beta_{e\_ave}^{(i-1)}, \quad a_2 = 20 f \cdot dt \end{array} \right. \quad (22a, b)$

$\left\{ \begin{array}{l} \tau_e^{(i)} = \beta_{e\_ave}^{(i)} \cdot G_e'(\omega_t^{(i)}) \cdot \gamma^{(i)} + \frac{G_e''(\omega_t^{(i)})}{\omega_t^{(i)}} \cdot \dot{\gamma}^{(i)} \\ \beta_{e\_ave}^{(i)} = \beta_e^{(i)} \cdot \gamma^{(i)} + (1 - a_2) \cdot \beta_{e\_ave}^{(i-1)}, \quad a_2 = 20 f \cdot dt \end{array} \right. \quad (23)$

$\left\{ \begin{array}{l} \tau_e^{(i)} = \beta_{e\_ave}^{(i)} \cdot G_e'(\omega_t^{(i)}) \cdot \gamma^{(i)} + \frac{G_e''(\omega_t^{(i)})}{\omega_t^{(i)}} \cdot \dot{\gamma}^{(i)} \\ \beta_{e\_ave}^{(i)} = \beta_e^{(i)} \cdot \gamma^{(i)} + (1 - a_2) \cdot \beta_{e\_ave}^{(i-1)}, \quad a_2 = 20 f \cdot dt \end{array} \right. \quad (24a, b)$

Fig.13 (a) and (b) are the hysteresis loops calculated by the above method, and the curves are better than that of Fig.11. The next section will show the hysteresis loops of other sine and random waves.

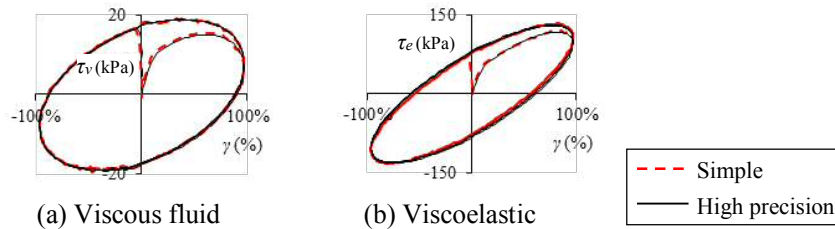


Fig. 13 – Hysteresis loops of each model after modifying (sine 0.25Hz, 20°C)

#### 4.4 Precision of simple model in time history analysis

This section shows the hysteresis loops calculated with the simple model and the high precision model in order to confirm the precision of the simple model of previous section. The input strains are sine waves and random waves the maximums strain of which are 100%. The frequencies of sine waves are 0.1, 2.5Hz. The random waves shown in Fig.14 are the first floor response displacements of 24, 3story buildings in JAM Kobe wave and El Centro wave.

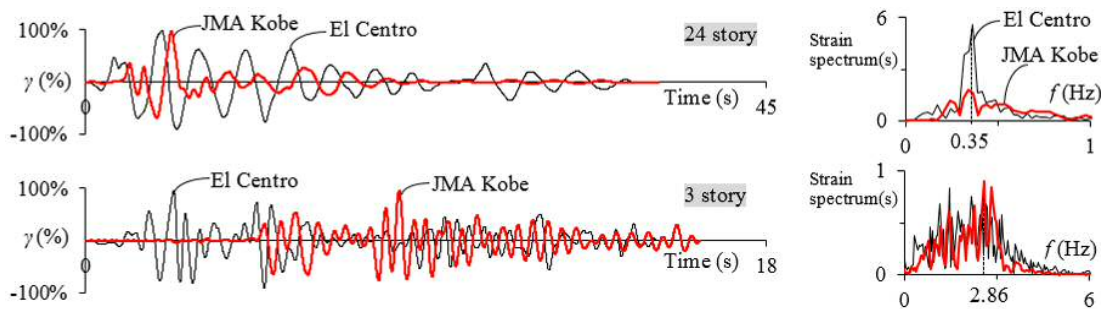


Fig. 14 – Time histories and spectrums of strain of random waves

Fig.15 shows the viscous fluid and viscoelastic hysteresis loops calculated with the simple model and the high precision model at 20°C. There are some differences at the first and third quadrants in some random waves. They are considered to regard as influence of the method of smooth and modify. However, the most values calculated by the simple model are consistent with that of the high precision model. It means that the accuracy of the simple model is very good. In addition, it is thought that this method can be applied to not only the series model of section 2.3 but also the non-linear characteristics of the viscoelastic mechanical model. However, they are the future tasks.

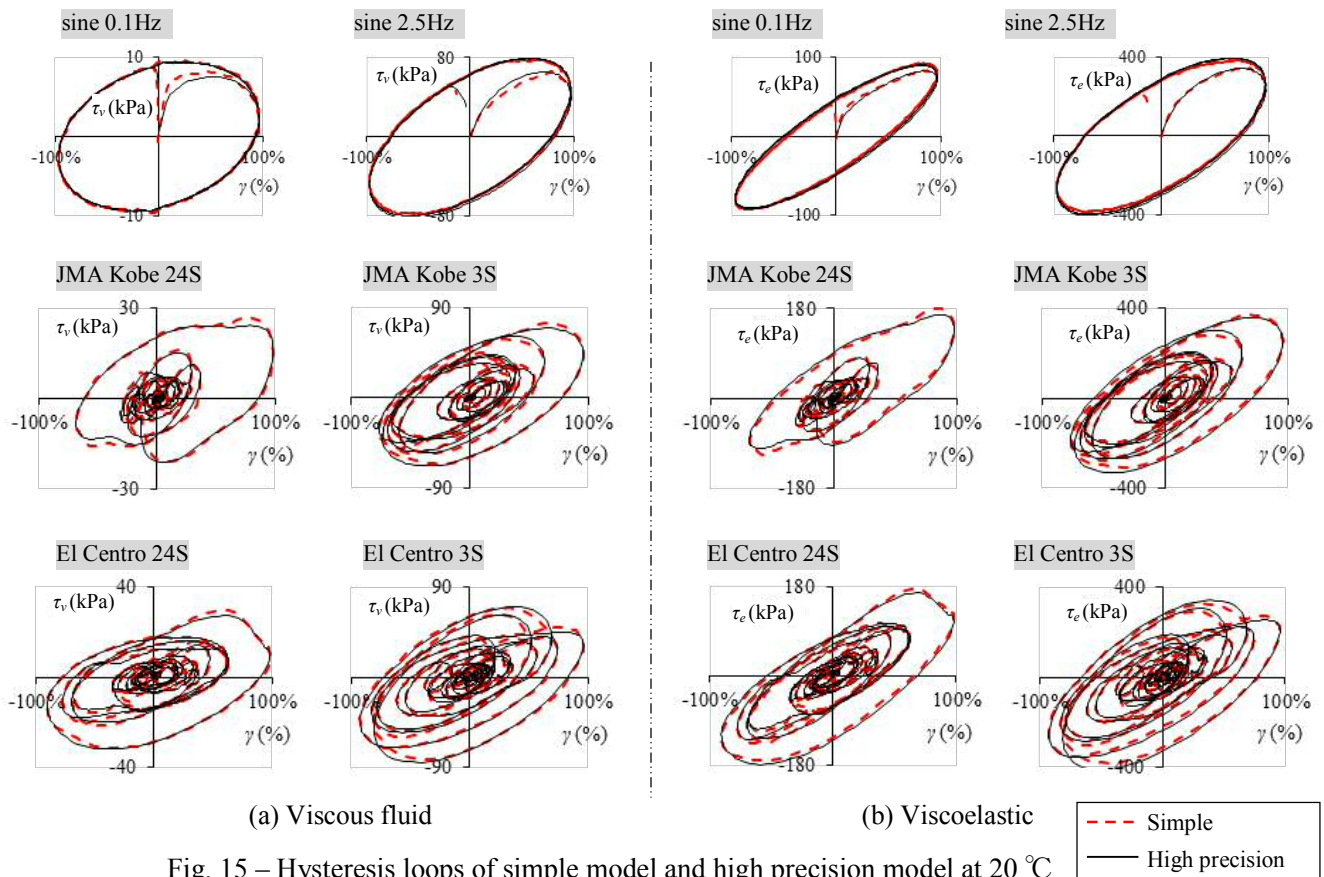


Fig. 15 – Hysteresis loops of simple model and high precision model at 20 °C

## 5. Summary

This paper explained about the simple model to calculate the linear characteristics of viscoelastic mechanical model for the viscous dampers and viscoelastic dampers with the instant circular frequent. It is described below.

- 1) It is important to smooth the strain and got smoothed strain acceleration in order to calculate the steady the instant circular frequent with the measured values.
- 2) It is necessary to modify the characteristics values in the condition that does not occur in logical sine wave.
- 3) Values calculated with the simple model mostly coincide with those of the high precision mode.
- 4) Though some differences of the values of the simple model and the high precision models there are, if the method to smooth and modify can be improved, it is considered that those differences will be smaller.
- 5) The simple model is considered to easily apply to the other more complex models.



## 6. References

- [1] Japan Society of Seismic Isolation (2013): *Manual for design and construction of passively-controlled buildings*, 3<sup>rd</sup> edition.
- [2] Sato, S., Ikenaga, M., Mochimaru, M., Kondo, T., Okabe, A., Suzuki, M. (1997): *High Velocity Test of Viscous Damping Wall*, Summaries of technical papers of annual meeting Architectural Institute of Japan, pp861-862.
- [3] Tsuchihashi, T., Kasai, K., Chaya, Y., Yasuda, M., Honma, T. (2013): *Analysis of Response Records from Advanced Protected Buildings in a District of Tokyo Shaken by the 2011 Tohoku Earthquake : Part3-Three Cases of Response Controlled Buildings*, Summaries of technical papers of annual meeting Architectural Institute of Japan, pp607-608.
- [4] Sasaki, K., Kasai, K., Ooki, Y., Wake, T. (2011): *EXPERIMENT METHOD AND GRASP OF DYNAMIC PROPERTIES OF VISCOUS FLUID MATERIAL: Study on strain, temperature and frequency sensitives dependence of shearing type viscous fluid damper Part1*, Transactions of AIJ. Journal of structural and construction engineering, No.670, pp2183-2192.
- [5] Sasaki, K., Kasai, K., Ooki, Y. (2012): *MODELING OF LINEAR PROPERTIES OF VISCOUS FLUID MATERIAL IN SMALL STRAIN: Study on strain, temperature and frequency sensitives dependence of shearing type viscous fluid damper Part2*, Transactions of AIJ. Journal of structural and construction engineering, No.675, pp791-298.
- [6] Sasaki, K., Kasai, K. (2013): *MACROSCOPIC AND SIMPLE NON-LINEAR MODELING OF VISCOUS FLUID MATERIAL UNDER LARGER STRAINS, temperature and frequency sensitivity dependence of shearing type viscous fluid damper Part3*, Transactions of AIJ. Journal of structural and construction engineering, No.685, pp607-615.
- [7] Soda, S., Takahashi, Y. (1997): *QUANTIFICATION OF FREQUENCY-DEPENDENT PROPERTY OF VISCO-ELASTIC DAMPER BY RANDOM LOADING METHOD*, Transactions of AIJ. Journal of structural and construction engineering, No.498, pp43-49.
- [8] Kasai, K., Teramoto, M., Okuma K., Tokoro, K. (2001): *CONSTITUTIVE RULE FOR VISCOELASTIC MATERIALS CONSIDERING TEMPERATURE, FREQUENCY, AND STRAIN SENSITIVITIES: Part 1 Linear model with temperature and frequency sensitivities*, Transactions of AIJ. Journal of structural and construction engineering, No.543, pp77-86.
- [9] Kasai, K., Tokoro, K. (2002): *CONSTITUTIVE RULE FOR VISCOELASTIC MATERIALS HAVING TEMPERATURE, FREQUENCY, AND STRAIN SENSITIVITIES: Part 2 Nonlinear model based on temperature-rise, strain and strain-rate*, Transactions of AIJ. Journal of structural and construction engineering, No.561, pp55-63.
- [10] Kasai, K., Ooki, Y., Amemiya, K., Kimura, K. (2003): *A CONSTITUTIVE RULE FOR VISCOELASTIC MATERIALS COMBINING ISO-BUTYLENE AND STYRENE POLYMERS: Part 1 Linear model considering temperature and frequency sensitivities*, Transactions of AIJ. Journal of structural and construction engineering, No.569, pp47-54.
- [11] Ooki, Y., Kasai, K., Amemiya, K., Kimura, K. (2007): *A CONSTITUTIVE RULE FOR VISCOELASTIC MATERIALS COMBINING ISO-BUTYLENE AND STYRENE POLYMERS: Part2 Non-linear model considering temperature, frequency, and strain sensitivities*, Transactions of AIJ. Journal of structural and construction engineering, No.617, pp77-85.
- [12] Huang, Y., Kato, T., Wada, A., Iwata, M., Takeuchi, T., Okuma, K. (1999): *THE DYNAMIC MECHANICAL MODEL OF VISCOELASTIC DAMPERS RELYING ON THE FREQUENCY AND TEMPERATURE*, Transactions of AIJ. Journal of structural and construction engineering, No.516, pp91-98.